INL/EXT-13-29551

A Variable Load LVDT-Based Creep Test Rig for Use in ATR Loop 2A

K. L. Davis
D. L. Knudson
J. L. Rempe
K. G. Condie

July 2013

The INL is a
U.S. Department of Energy
National Laboratory
operated by
Battelle Energy Alliance

INL/EXT-13-29551

A Variable Load LVDT-Based Creep Test Rig for Use in ATR Loop 2A

K. L. Davis, D. L. Knudson, J. L. Rempe, and K. G. Condie

July 2013

Idaho National Laboratory
Idaho Falls, Idaho 83415

Prepared for the
U.S. Department of Energy
Office of Nuclear Energy
Under DOE Idaho Operations Office
Contract DE-AC07-05ID14517

CONTENTS

FIGURES

TABLES

1. INTRODUCTION

Understanding the creep behavior of materials in a radiation environment is essential in evaluating safety issues associated with nuclear power plant operation, especially for plants applying for life extension. In US materials testing reactors (MTRs), this understanding has been achieved through a "cook and look" approach (where specimens are irradiated under load for some period of time and then removed from an MTR for post-irradiation examination). A number of "cook and look" cycles can be required for each evaluated material, which makes this approach expensive. In addition, examinations are limited to end-state conditions, which may or may not be sufficient to reveal all phenomena of interest (because examinations are not performed at prototypic conditions relative to temperature, pressure, stress, etc.).

A creep test rig that facilitates real-time in-pile measurement of material creep behavior in the Advanced Test Reactor (ATR) has been developed.[1] This rig was designed with an externally-pressurized bellows to load a tensile specimen coupled with a linear variable displacement transformer (LVDT) used to detect material creep. This test rig is simple in design and easy to deploy, but it is limited in that it can only apply a load that corresponds to the external pressure of the coolant in the ATR pressurized water reactor (PWR) loop.

It is unlikely that the primary damage experienced by a specimen will be the result of the applied stress during irradiation. Even so, the subsequent process of dislocation formation, that is responsible for radiation hardening, yield drop, and plastic flow localization, will be substantially altered by the applied stress. Furthermore, it is speculated that the fatigue lifetime during in-situ cyclic loading experiments may be significantly different from the ones obtained during fatigue experiments on specimens in the post-irradiated condition.[2] For these reasons, the INL developed the Variable Load Creep Test Rig based upon the design of the creep test rig discussed in Reference [1]. The Variable Load Creep Test Rig will provide for variable strain rate testing, fatigue testing and will allow for a larger selection of test materials. It is also similar in function to another creep test rig, [3,4] but its design combines the load path and displacement detection into one simplified structure.

Efforts required to qualify the Variable Load Creep Test Rig for deployment in Loop 2A of the ATR are discussed in this document. Specifically, background information is provided in Section 2 relative to the ATR, ATR Loop 2A, LVDT operation, and the international use of creep test rigs. Section 3 contains a description of the Variable Load Creep Test Rig as designed for Loop 2A deployment. Characterization of the bellows relative to the effective area and spring rate is outlined in Section 4, while calibration of the LVDT as a function of temperature is described in Section 5. Finally, a summary and pertinent references are provided in Sections 6 and 7, respectively.

2. BACKGROUND

Information is provided in this section to assist with understanding the ATR and Loop 2A within this MTR (see Section 2.1), the basics of LVDT operation (see Section 2.2), prior LVDT evaluations (see Section 2.3), and the international use of creep test rigs in various MTRs (see Section 2.4).

2.1. ATR

The ATR is a unique facility designed for evaluating the effects of radiation on nuclear fuel and materials. The reactor has a maximum power rating of 250 MW_{th} with a maximum unperturbed thermal neutron flux of $1x10^{15}$ n/cm^2-s and a maximum unperturbed fast neutron flux of $5x10^{14}$ n/cm^2-s, which allows accumulation of high neutron exposure in a shorter time period than possible with many other MTRs. The ATR is cooled by pressurized (2.5 MPa) water that enters the reactor vessel bottom at an average temperature of 52 °C, flows up outside cylindrical tanks that support and contain the core, passes through concentric thermal shields into the open part of the vessel, then flows down through the core to a flow distribution tank in the bottom of the vessel. When the reactor is operating at full power, the primary coolant exits the core at 71 °C.

As shown in Figure 2-1, the 122 cm tall ATR core consists of 40 curved plate fuel elements configured in a serpentine arrangement around a 3x3 array of nine primary testing locations (known as the neutron flux traps). A unique ATR control device permits power variations among the nine flux traps using a combination of control drums and neck shim rods. Within bounds, the power level in each corner lobe of the reactor can be controlled independently to allow for different power and flux levels in the ATR core during a single operating cycle. Using specialized test capsule liners, the ratio of fast to thermal flux can also be varied from 0.1 to 1.0. In addition to the nine neutron flux traps, there are 66 irradiation positions inside the reactor core reflector tank and 34 low-flux irradiation positions in two capsule irradiation tanks outside the core.

The Loop 2A Reactivation Project was initiated by Battelle Energy Alliance in 2005 to restore an ATR pressurized water loop capability that had been deactivated for more than a decade. Bolstering nuclear research capabilities at the INL was a prime motivator for restoration of the loop, which was completed in 2012 as part of the National Scientific User Facility (NSUF) program. As indicated in Figure 2-2, Loop 2A includes pumps, heaters, a pressurizer, and all other related piping and equipment to allow full control of loop flows, temperatures, pressures, and water chemistries. The loop resides in the center flux trap of the ATR with remotely-located operating consoles to enable loop control and data collection. Selected outputs from the operating consoles are available for monitoring by off-site researchers.

In this effort, a test rig for real-time in-pile measurement of material creep behavior has been designed and developed specifically for Loop 2A deployment. The design is based on the use of an differentially-pressurized bellows to load a specimen with an LVDT to detect material creep. Complete details associated with the design are outlined in Section 3.

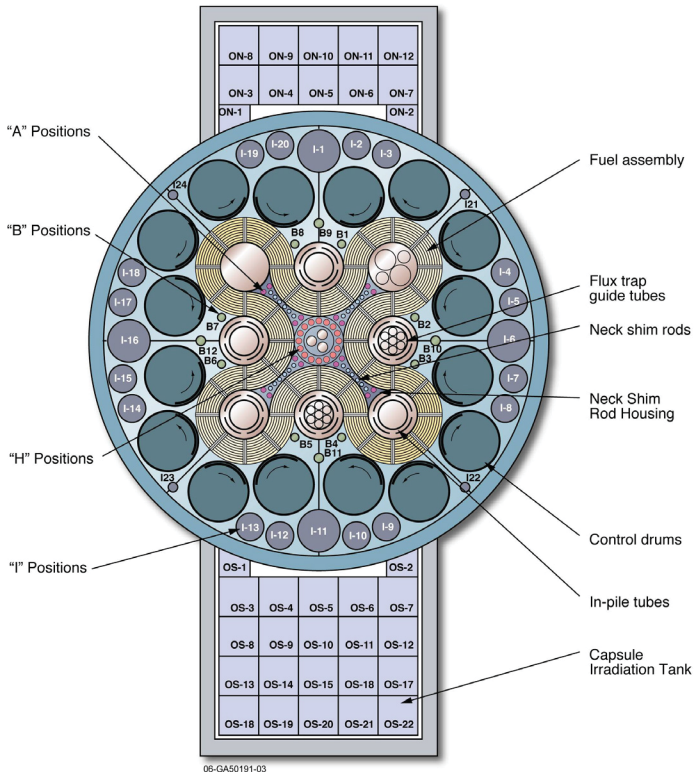

Figure 2-1. ATR core cross section showing irradiation locations.

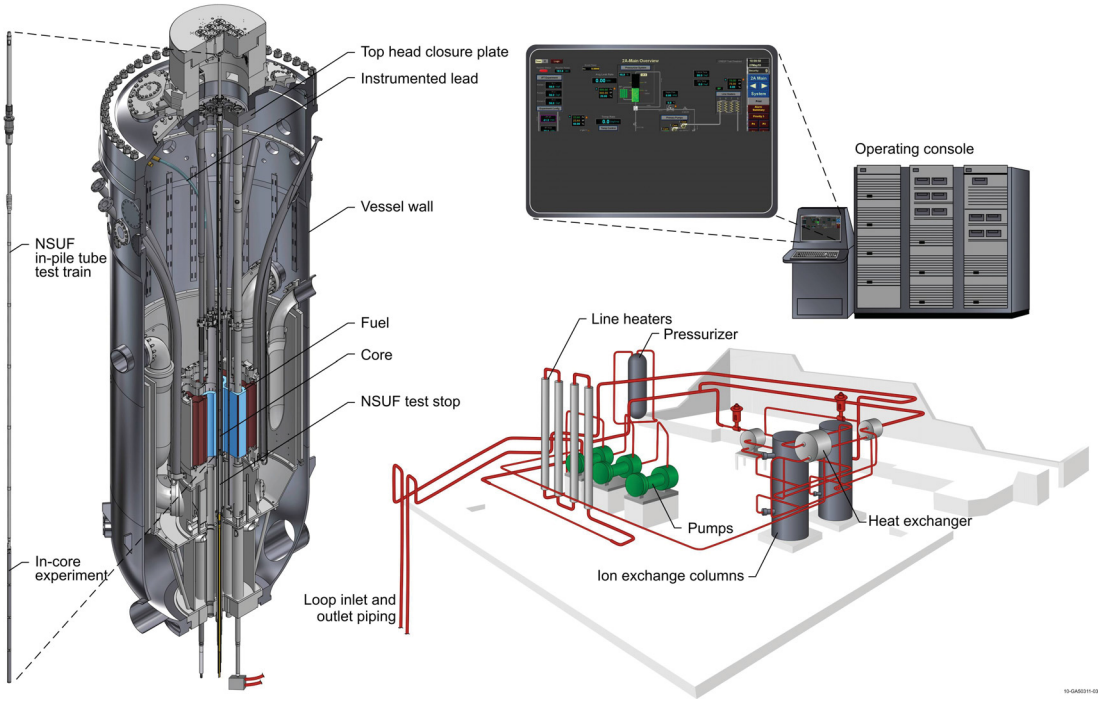

Figure 2-2. ATR Loop 2A schematic.

2.2. LVDT Operation

LVDTs are simple, reliable, inexpensive devices that convert the mechanical movement of a specimen into an electrical output. A cross-section of a basic LVDT design is shown in Figure 2-3. As indicated, a magnetically-permeable core is attached to a specimen. The core then moves inside a tube in response to any change in specimen length or position. Three coils are wrapped around the tube: a single primary coil and two secondary coils.

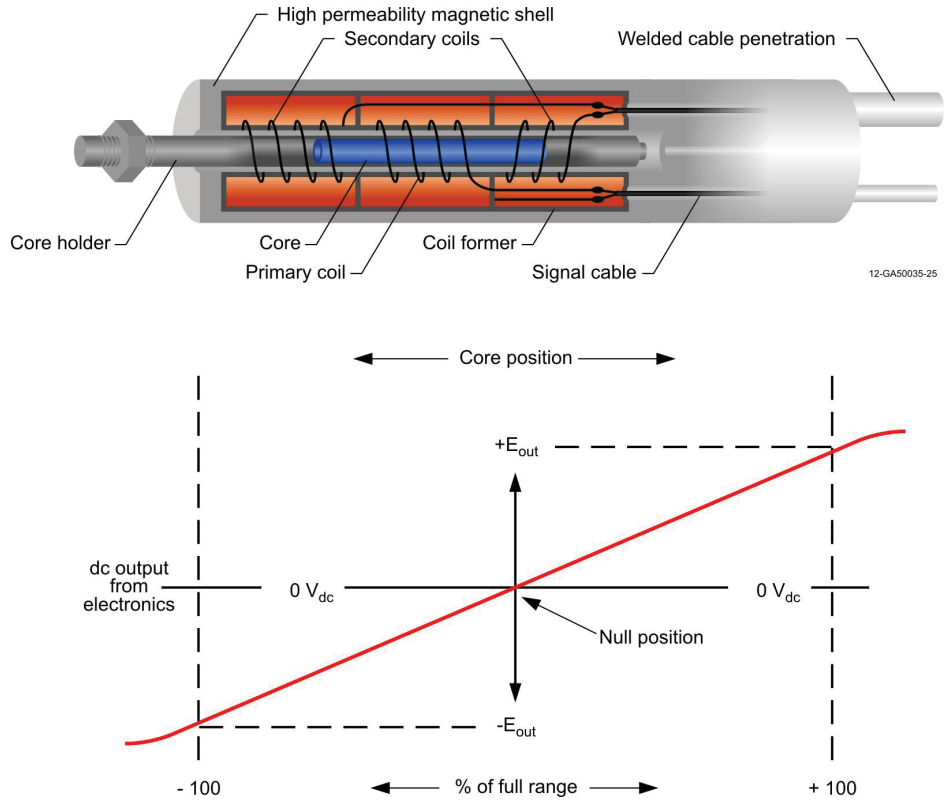

Figure 2-3. LVDT design and operation.

To operate the LVDT, an alternating (excitation) current is driven through the primary coil, causing a voltage to be induced in each secondary coil, which is proportional to its mutual inductance with the primary. As the specimen and the attached core moves, these mutual inductances change, causing voltages induced in the secondaries to change. The secondary coils are connected in reverse series, so that an output voltage can be conveniently derived from the difference between the two secondary voltages. Specifically, when the core is in its central position (equidistant between the two secondaries), equal but opposite voltages are induced in the secondary coils so the output voltage is zero. When the core is moved to its full scale mechanical position (in either the positive or negative direction), a corresponding output voltage (either positive or negative) is registered as the voltage induced in one of the secondary coils goes full scale while the voltage in the other secondary coil goes to zero. (See Figure 2-3.)

2.3. Prior LVDT Evaluations

Although LVDTs are simple devices, it was necessary to identify instruments capable of reliably operating within the ATR environment. To this end, five major efforts have been completed: (1) a comparison of the high temperature behavior of candidate nuclear-grade LVDTs, (2) an assessment of Curie temperature effects in the selected LVDT, (3) a gamma heating analysis to determine allowable positions in the ATR core for the selected LVDT, (4) a high temperature evaluation of the selected LVDT with an alternate coil material, and (5) an autoclave evaluation of the selected LVDT to verify elongation measurement accuracy at high temperatures and pressures. Those efforts are documented in References [5], [6] and [7].

2.4. Test Rigs at International MTRs

References [8], [9] and [10] and describe prior efforts by several research organizations to deploy creep test rigs in various MTRs [e.g., the Technical Research Organization of Finland (VTT) to deploy a rig in the Belgium Reactor 2 (BR2), the Korean Atomic Energy Research Institute (KAERI) to deploy a rig in HANARO, the Japan Atomic Energy Research Institute (JAERI) to deploy a rig in the Japan Material Test Reactor (JMTR), the Institute for Energy Technology at the Halden Research Project (IFE/HRP) at the Halden Boiling Water Reactor (HBWR), the French Atomic Energy Commission (CEA) to deploy a rig in OSIRIS, and the Nuclear Research and Consultancy Group (NRG) to deploy a rig in the High Flux Reactor (HFR)]. Selected aspects of these various creep test setups are compared in Table 2-1.[8] In most cases, test pressures external to the bellows are offset by internal bellows pressurization to produce the variable loads. As indicated, however, most of the setups are designed to test specimens in inert gas. A notable exception is specimen testing in reactor coolant conducted in BR2 which would be the most comparable to the Variable Load Creep Test Rig documented in this report. The creep test rig used in BR2 is illustrated in Figure 2-4 (courtesy of Ref. 3).

Table 2-1. Summary of creep testing in MTRs.

Country/MTR/Research Organization	Test Conditions	Real Time Load Control	Method	Real Time Elongation Detection	Method
Belgium/BR2/VTT	Stagnant reactor coolant (~ 90 °C)	Yes	Internally pressurized bellows	Yes	Monitored LVDT
France/OSIRIS[a]/CEA	Inert gas, water, and NaK (from room temperature up to 380 °C)	Yes	Internally pressurized bellows	Yes (also external diameter gauges)	Monitored LVDT
Norway/HBWR/(IFE/HRP)	Inert gas (240-400 °C)	Yes	Internally pressurized bellows	Yes (also external diameter gauges)	Monitored LVDT (under development for 600 °C and 250 bar)
Japan/JMTR/JAERI	Inert gas (550 °C)	Yes	Internally pressurized bellows	Yes	Monitored LVDT
Netherlands/HFR/NRG	Inert gas and NaK (300-600 °C)	Yes	Self-contained spring-washer system	Yes (semi-continuous)	Monitored LVDT
Korea/HANARO/KAERI	Inert gas (up to 600 °C)	Yes	Internally pressurized bellows	Yes	Monitored LVDT

a. In upcoming tests. Previous tests relied on out-of-pile measurements with strain gauges.

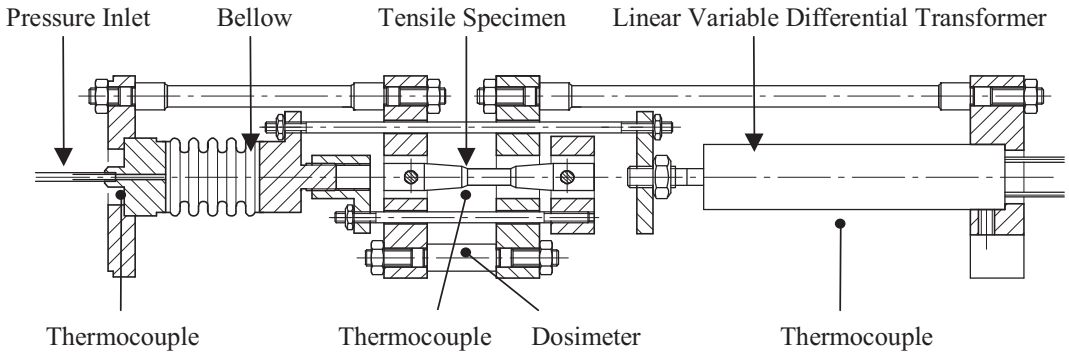

a)

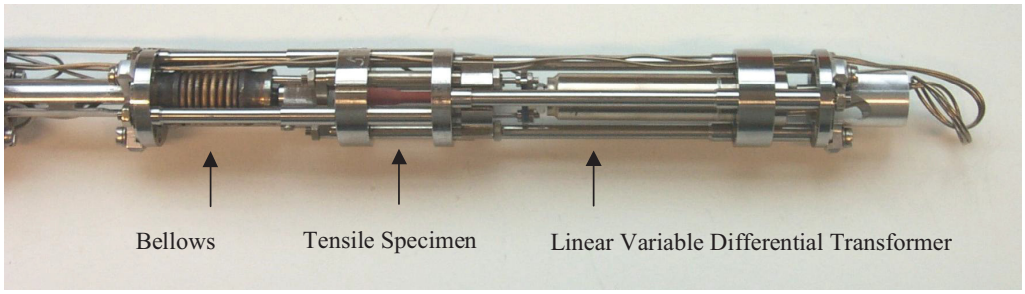

b)

Figure 2-4. VTT Controlled Load Creep Test Rig (a) the simplified layout and operational features including the necessary instrumentation of the test module and (b) the final assembly of the complete test module before installation in the irradiation rig.

3. CREEP TEST RIG

The Variable Load Creep Test Rig was designed and fabricated for deployment in ATR Loop 2A. This test rig is a refinement of an initial INL-developed creep test rig design.[1] Details are provided below.

The Variable Load Creep Test Rig consists of two major components: the LVDT assembly and the LVDT fixture. The LVDT assembly includes the LVDT (manufactured by IFE/HRP) and the probe assembly (manufactured by INL). The LVDT body is made of Inconel 600 with silver alloy wire used in the construction of the coils. The probe assembly, as shown in Figure 3-1, consists of an LVDT core inside a housing, a bellows, and connecting hardware. Most of the probe assembly was made from Inconel 600 with the exception of the core (Type 5 provided by IFE/HRP) and the bellows (Inconel 718 provided by Miniflex Corporation). The housing with connecting hardware provides the mechanism to connect movement of a specimen to movement of the LVDT core as the bellows contracts (or expands). To minimize costs, all components of the Variable Load Creep Test Rig were designed to be interchangeable with the initial creep test rig. All testing and calibration was conducted using the original hardware designed for the initial creep test rig. Characteristics of the bellows are given in Table 3-1. The (complete) LVDT assembly is shown in Figure 3-2.

The LVDT fixture includes a frame and associated hardware to connect the LVDT assembly to a creep specimen. The fixture is designed to constrain the LVDT assembly and one end of the specimen so that bellows contraction will place the specimen in tension. With respect to Figure 3-3, the LVDT fixture is everything shown except the LVDT assembly.

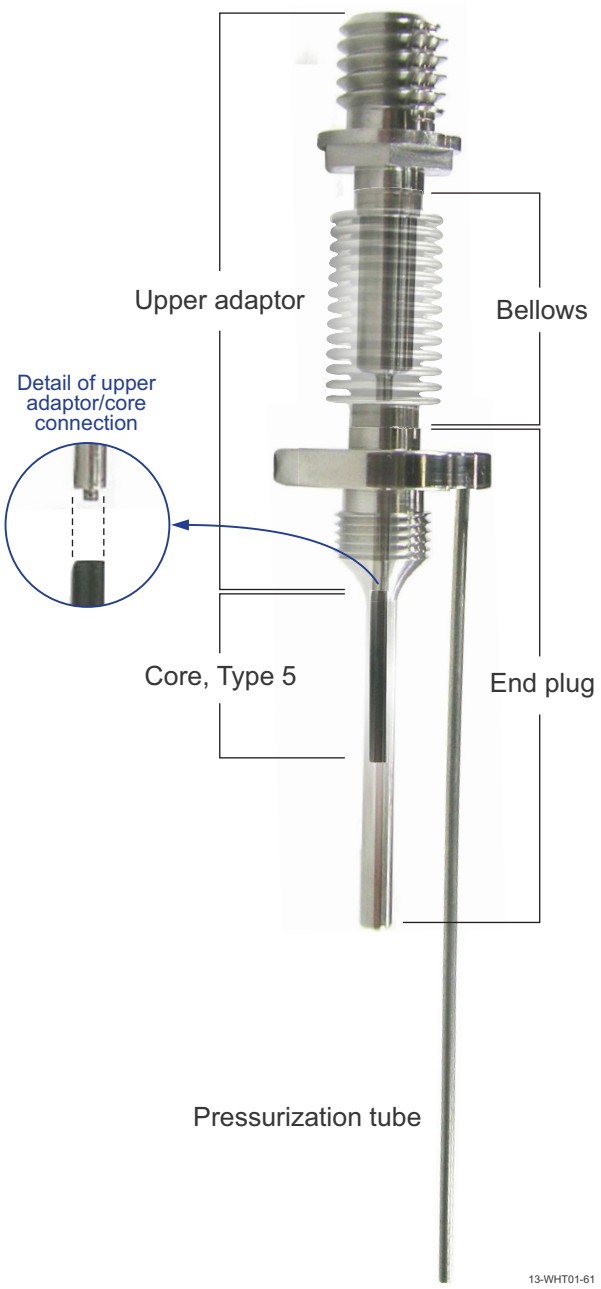

Figure 3-1. The probe assembly (laser welding was used to attach the core to the upper adaptor, the bellows to the upper adaptor and end plug and the pressurization tube to the end plug).

Table 3-1. Bellows specifications.

Item	Value
Convolution ID (mm)	7.19
Convolution OD (mm)	13.0
Wall thickness (mm)	0.279
Effective area (mm^2)	79.4
Neck OD (mm)	8.17 ± 0.0127
Neck ID (mm)	7.58 ± 0.0127
Neck length (mm)	3.34 ± 0.419
Number of convolutions	13
Convolution free length (mm)	21.3
Maximum deflection in compression (mm)	3.71
Spring rate (N/mm)	138 (175 after aging)
Squirm rating (MPa)	26.2 (39.3 after aging)
Burst rating (MPa)	55.2 (72.4 after aging)
Comments	Inconel 718, procured 10/29/08

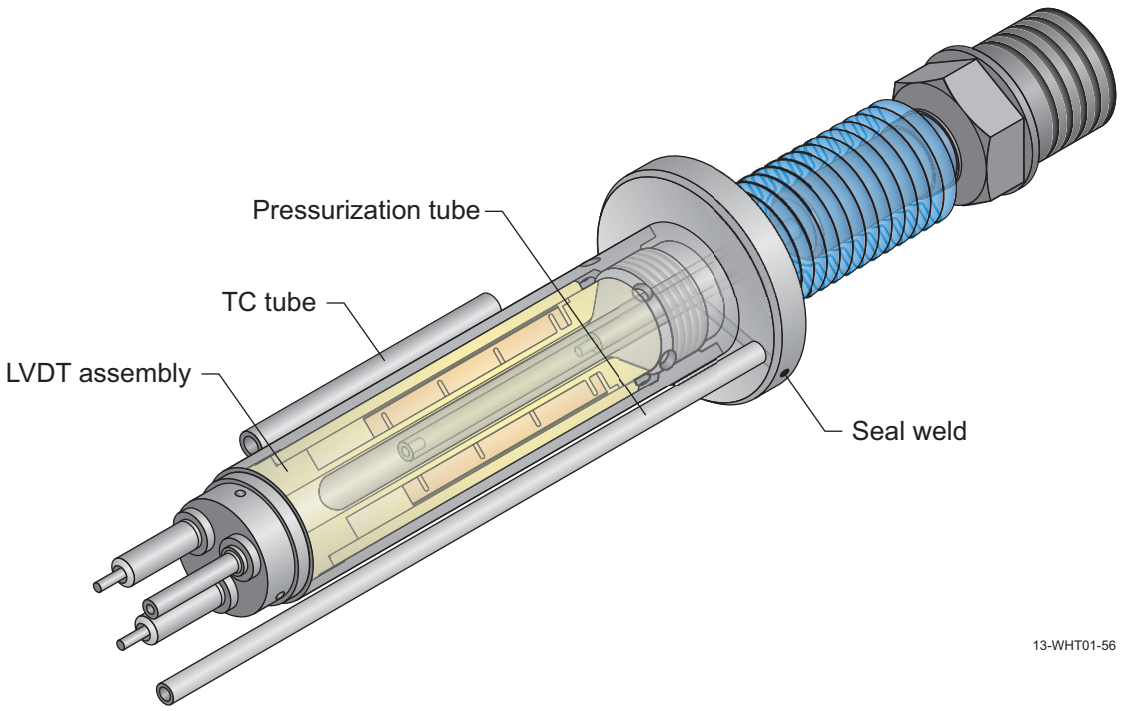

Figure 3-2. LVDT assembly.

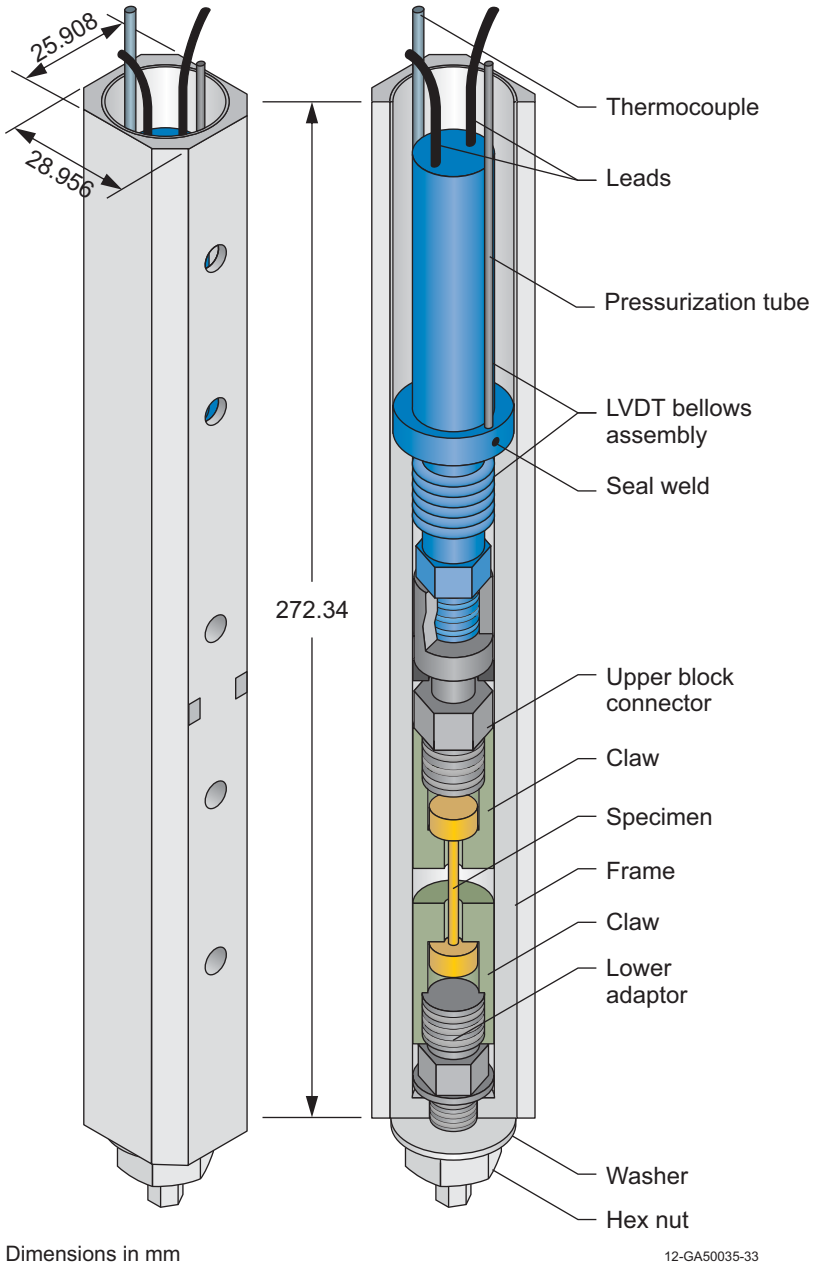

Figure 3-3. Creep test rig.

4. CHARACTERIZATION

The bellows spring rate and effective area were characterized so that the load applied to a specimen can be quantified. This section describes the characterization process.

Based on the configuration shown in Figure 4-1, the specimen load (F_S) is given by

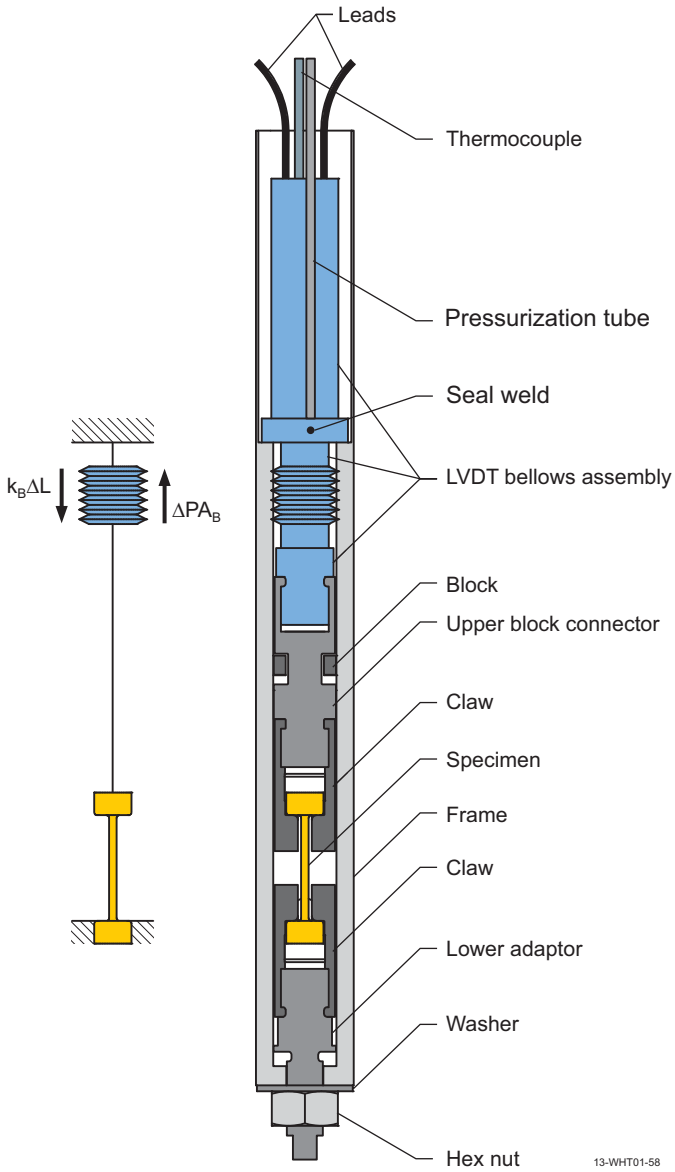

Figure 4-1. Test configuration with an equivalent specimen load diagram.

$$F_s = \Delta P A_B - k_B \Delta L \tag{4-1}$$

where

ΔP = differential pressure ($P_{external} - P_{internal}$) acting on the bellows effective area,
A_B = bellows effective area,
k_B = bellows spring rate,
ΔL = displacement of the bellows (and the specimen) as detected by the LVDT.

Once the spring rate and effective area have been characterized, the specimen load can be readily determined as a function of pressure and displacement measurements using Equation (4-1). Spring rate and effective area characterization required use of the fixture described in Section 4.1. Section.

4.1. Characterization Fixture

The characterization fixture consisted of the components shown in Figure 4-2. The spring rate and the effective area were determined with this fixture, using an appropriate bolt adaptor. Both bolt adaptors have an internal thread on one end to mate with the load cell. However, the opposite ends of the bolt adaptors differ. Specifically, the bolt adaptor used to determine the spring rate has a cup large enough to allow the allen bolt to freely slide inside, while the adaptor used to determine the effective area has an internal thread to mate with the allen bolt. (Note that the probe assembly is threaded into the LVDT to complete the LVDT assembly shown in Figures 3-1 and 3-2.) More detailed information regarding the use of the fixture to characterize the bellows is provided in subsequent sections.

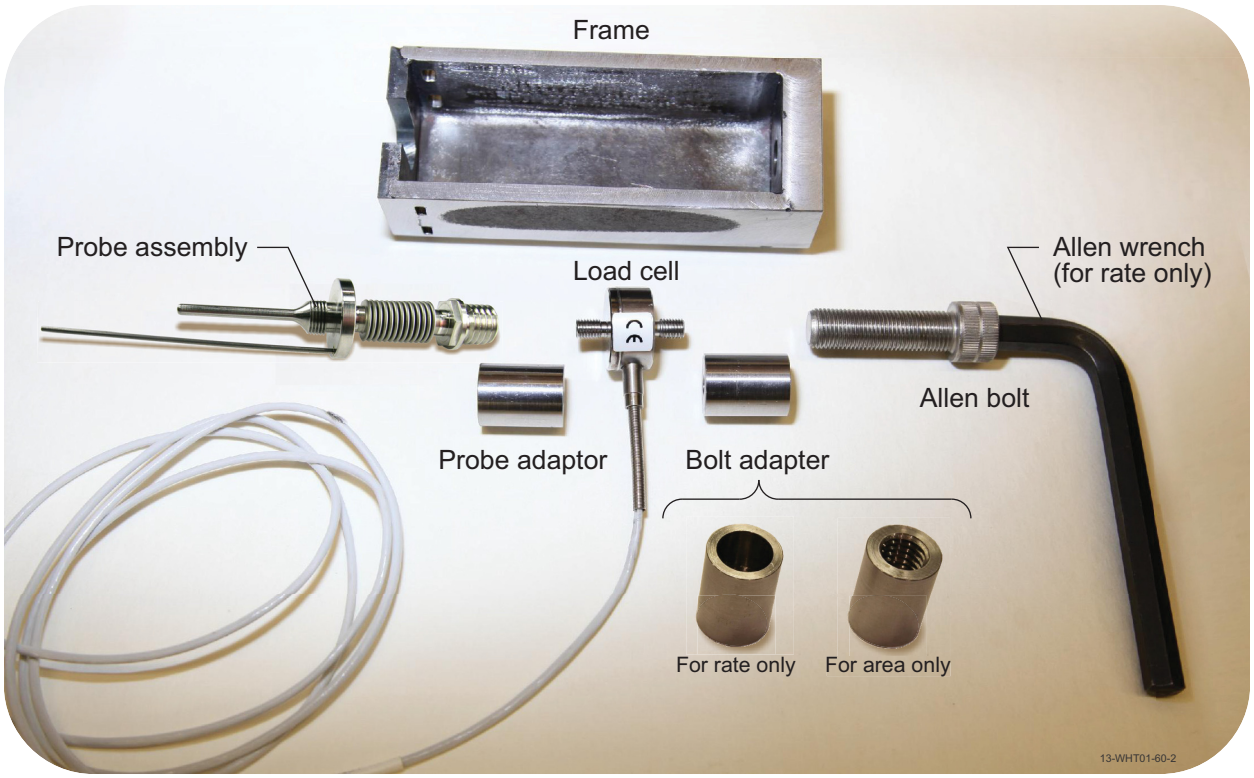

Figure 4-2. Components of the characterization fixture.

4.2. Bellows Spring Rate

The bellows spring rate was determined through a series of bench top measurements using the fixture configuration shown in Figure 4-3. In this case, the probe assembly was constrained by one end of the frame so that the bellows could be collapsed by incrementally tightening the allen bolt into threads in the opposite end of the frame. Note that the adaptor mating with the allen bolt is not threaded (as previously explained) so the bolt simply pushed that adaptor toward the bellows with each rotation. As the allen bolt was tightened, an ever increasing force was registered by the (calibrated) load cell consistent with the bellows spring rate and displacement. Displacement of the bellows was periodically measured during incremental bolt tightening, using a depth micrometer. The depth micrometer was clamped in line with the spring rate fixture and the micrometer was simply advanced to touch the head of the hex bolt each time the bolt was tightened as indicated in Figure 4-4.

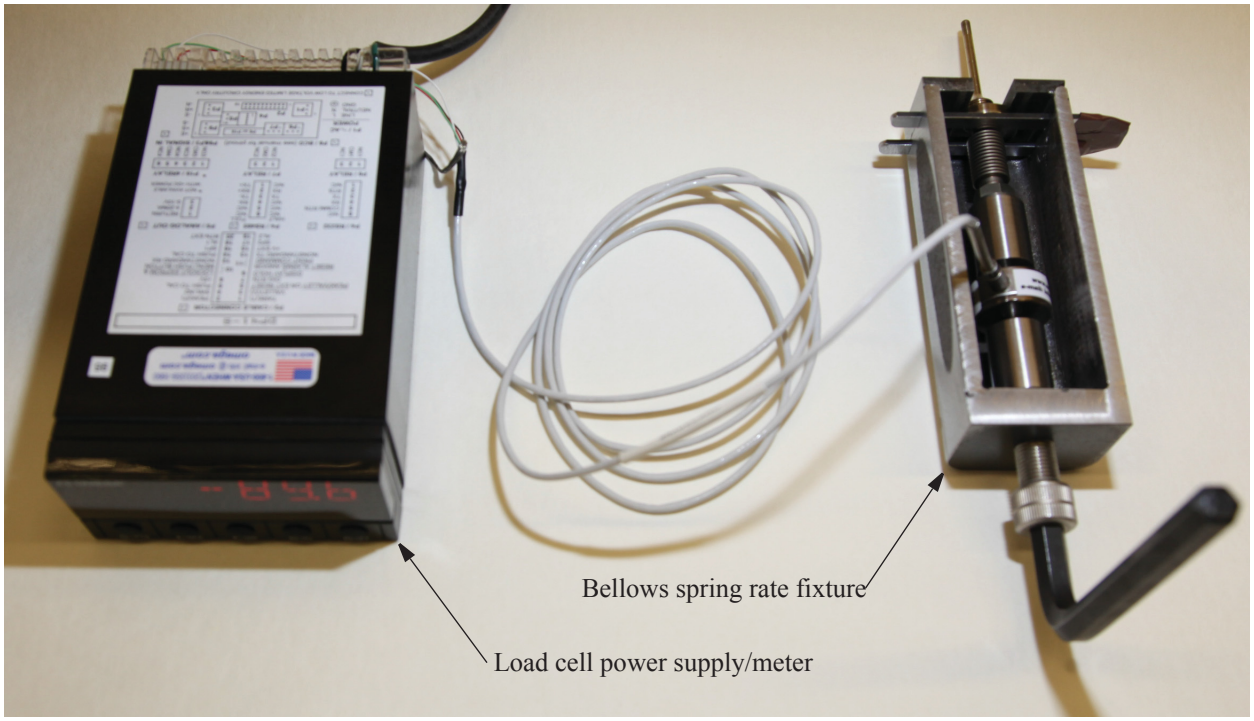

Figure 4-3. Bellows spring rate test setup. Note: components of the Variable Load Creep Test Rig were designed to be interchangeable with the initial creep test rig. The probe assembly shown is from the initial creep test rig.

The spring rate characterization process consisted of incrementally tightening the allen bolt, recording the load cell output, and measuring the associated displacement. That process was repeated until the total displacement of the bellows reached ~2.5 to ~3 mm. (Displacement of 2.5 to 3 mm was sufficient to exercise the bulk of the bellows allowable travel without pressing the travel limit of 3.7 mm.) Relative to Equation (4-1), ΔP was effectively zero and (F_S) was registered through the load cell while ΔL was measured. That allowed direct calculation of the bellows spring rate (k_B) based on the measured values. Results from this effort are summarized in Table 4-1. (Note that all bench top measurements were completed at room temperature with the assumption that the spring rate is temperature independent.)

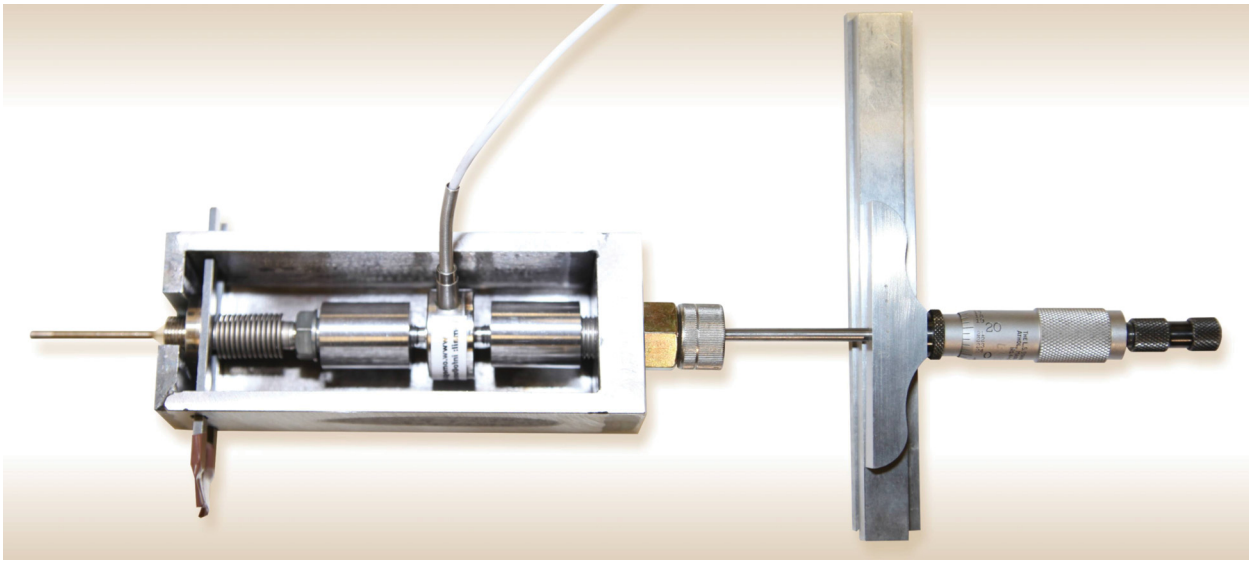

Figure 4-4. Depth micrometer configuration (without clamps) for measurement of the bellows spring rate. Note: components of the Variable Load Creep Test Rig were designed to be interchangeable with the initial creep test rig. The probe assembly shown is from the initial creep test rig.

Table 4-1. Bellows spring rate measurement summary.

Test	Spring Rate (N/mm)[a]
SR1	137
SR2	137
SR3	138

a. From a best-fit linear approximation of the measured data.

Results from these test are provided in Table 4-1. Shown in Figure 4-5 are the data from Test SR1 and the best-fit linear approximation of the measured data. From Table 4-1, the average bellows spring rate is 137 N/mm. This result compares well with the manufacturer's reported nominal spring rate of 138 N/mm for bellows that have not been age hardened.

4.3. Bellows Effective Area

The bellows effective area was determined through a series of measurements in an argon atmosphere in an autoclave using a configuration very similar to that shown in Figure 4-3. In this case, however, the frame and the threaded bolt adaptor (see Figure 4-2) were used to eliminate all movement of the bellows. As autoclave pressures were increased, the (constrained) bellows imparted an ever increasing force in the (calibrated) load cell. Internal pressure in the bellows was varied during testing to verify proper design performance.

The effective area characterization process consisted of incrementally increasing or decreasing internal and external pressures while recording pressures along with the associated load cell output. The expansion

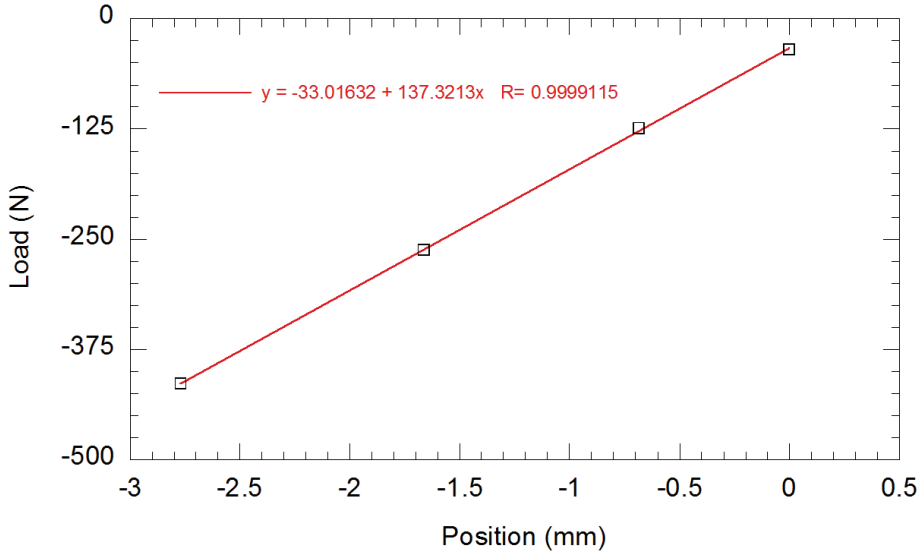

Figure 4-5. Bellows spring rates based on micrometer measurements in Test SR1.

of the bellows could result in plastic deformation, thus the internal pressure was never allowed to exceed the external pressure. A load limit of 1050 N was observed during testing (the load cell has a limit of ~1100 N.) Relative to Equation (4-1), ΔL was held at zero while (F_S) was registered through the load cell, and both external and internal pressures were measured. That allowed direct calculation of the bellows effective area (A_B) based on the measured values. Results from this effort are summarized in Table 4-2. (Note that all autoclave measurements were completed at room temperature because it is assumed that the effective area is temperature independent.) The bellows average effective area was found to be 78.3 mm^2. Relative to the manufacturer's reported area of 79.4 mm^2, this measured discrepancy (of ~1%) is believed to be well within normal manufacturing tolerances.

Table 4-2. Bellows effective area measurement summary.

Test	Load (N)	External Pressure (MPa)	Internal Pressure (MPa)	Area (mm^2)
EA1	259.3	3.4	0	75.2
	543.1	6.9	0	78.8
	850.0	10.6	0	80.1
	1004.4	12.7	0	79.2
	1053.3	13.1	0	80.4
	775.7	13.1	3.4	80.4
	496.8	13.1	6.9	80.1
	218.8	13.1	10.3	79.4
	513.3	13.1	6.9	82.7
	790.9	13.1	3.4	81.9
	1049.7	13.1	0	80.1
	759.7	13.1	3.4	78.7
	482.6	13.1	6.9	77.8
	205.9	13.1	10.3	74.7
	490.2	13.1	6.9	79.0
	778.4	13.1	3.4	80.6
	1037.3	13.1	0	79.2
	823.3	10.4	0	79.1
	532.0	6.9	0	77.2
	251.3	3.4	0	72.9
EA2	250.9	3.4	0	72.8
	545.3	7.1	0	76.8
	819.3	10.3	0	79.2
	535.1	10.3	3.4	77.6
	263.3	10.3	6.9	76.4
	568.9	10.4	3.4	81.7
	829.6	10.4	0	79.7
	528.4	6.9	0	76.6
	251.3	3.4	0	72.9

5. CALIBRATION

The LVDT bellows assembly must be calibrated over the range of temperatures that could be expected during deployment in the ATR Loop 2A. This required calibration provides the means to relate any measured LVDT output voltage to a corresponding displacement. Because internal pressure in the bellows assembly was not required, the internal pressure line was capped during calibration.

Calibration was completed at room temperature and at 150, 250, and 350 °C. This temperature range is expected to adequately cover operating conditions of interest during ATR deployment. Bench top and autoclave calibrations at room temperature were completed. Bench top measurements (at room temperature) provided a way to check results that were subsequently obtained through (room temperature) autoclave testing. That way, a degree of confidence was achieved relative to the validity of all autoclave testing, which was the only practical method to obtain higher temperature calibration results. Complete details associated with this calibration effort are discussed in the remainder of this section.

5.1. Setup

Because calibration was completed on the bench top as well as in an autoclave, bench top and autoclave setups were required as described below.

5.1.1. Bench Top

The bench top setup was essentially identical to the setup shown in Figure 4-4. The addition of the LVDT to the end of the probe assembly was the only difference. With the LVDT in place, each advancement of the allen bolt (which was measured with the depth micrometer) was accompanied by a change in the LVDT output voltage. The bench top calibration process consisted of incrementally tightening the allen bolt, recording the LVDT output voltage, and measuring the associated displacement. That process was repeated until the total displacement approached ~2.5 mm (which is within the bellows travel limit of 3.7 mm).

5.1.2. Autoclave

Autoclave testing was considerably more complex than bench top testing because of difficulties in measuring displacement inside the autoclave. Those difficulties were addressed through the design and fabrication of a specialized fixture with positive mechanical stops to accurately define a displacement. Components in that fixture are shown in Figure 5-1. The assembled fixture is shown in Figure 5-2.

The calibration fixture is assembled by first threading the probe assembly into the LVDT. The travel adapter is then threaded onto the bottom of the probe assembly, and the extender is threaded onto the bottom of the travel adapter. Those assembled components are then lowered inside the frame to a point where the flange on the probe assembly rests on a shoulder internal to the frame. The frame shoulder is positioned so that the top of the travel limiting recess (in the travel adapter) is just slightly above the travel block slots in the frame. After the travel blocks are inserted in the travel block slots, the spring and spring plates are stacked on the bottom of the frame and secured with the retaining and lock nut (see Figure 5-2).

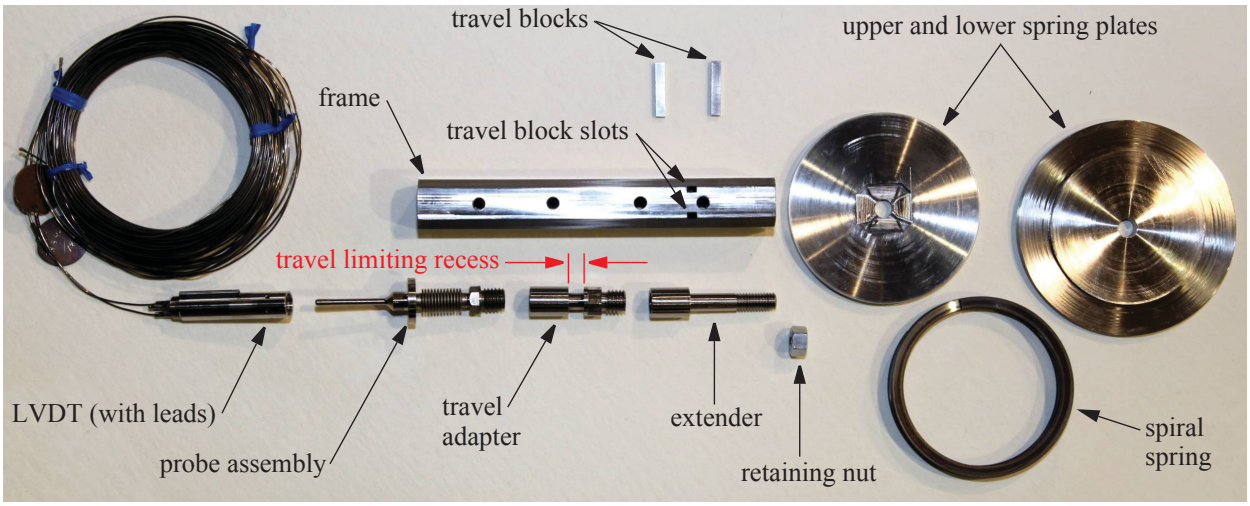

Figure 5-1. Autoclave calibration fixture components. Note: components of the Variable Load Creep Test Rig were designed to be interchangeable with the initial creep test rig. The probe assembly shown is from the initial creep test rig.

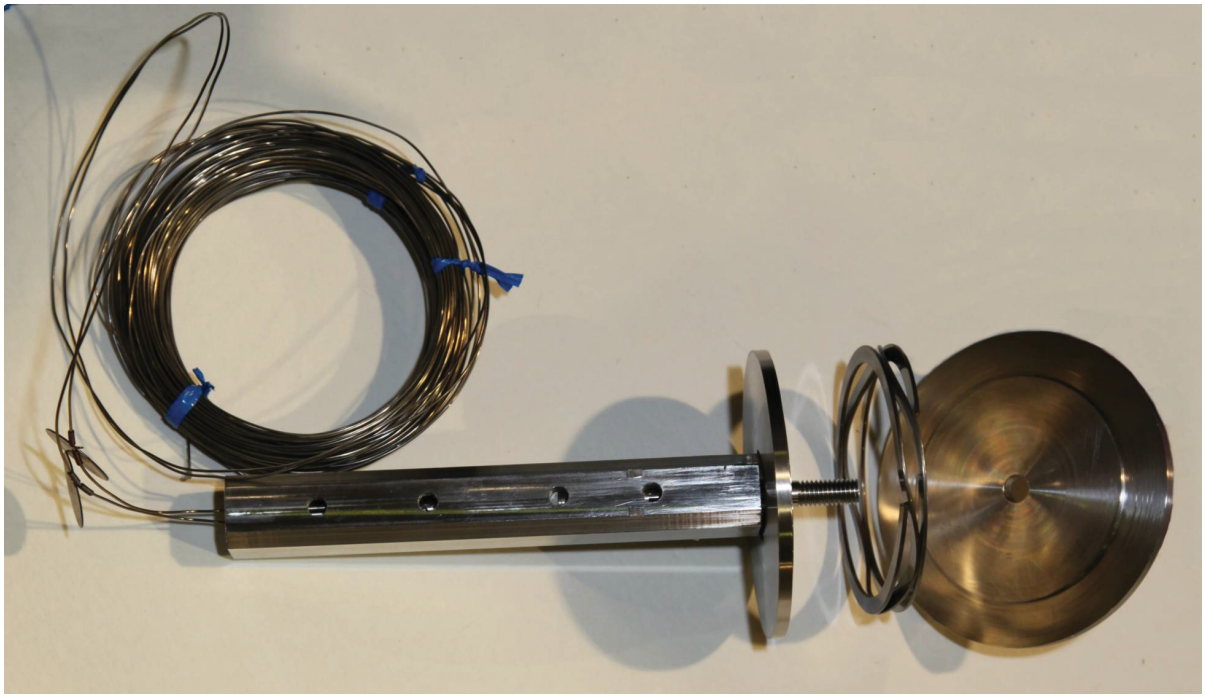

Figure 5-2. Autoclave calibration fixture.

At this point, the retaining nut can be tightened (and secured with a lock) just enough to (slightly) stretch the bellows and pull the top of the travel limiting recess (in the travel adapter) into contact with the travel blocks. That provides the initial position of the LVDT for all autoclave testing. As the pressure is increased during each test, the bellows contracts, which collapses the spiral spring and allows movement of the travel adapter. At some autoclave pressure, bellows contraction is sufficient for the bottom of the traveling limit recess to contact the travel blocks, which defines the final LVDT position for all autoclave test-

ing. (Note that the travel limit is the difference between the travel limit recess of 7.34 mm and the travel block height of 5.08 mm for a total of 2.26 mm, which is within the bellows limit of 3.7 mm.)

All autoclave calibration testing was conducted in a pressurized argon or nitrogen environment where autoclave heaters were used to achieve the desired temperature for each test. This was deemed to be the most practical way to complete the calibration as a function of temperature. Results from this effort are discussed below.

5.2. Results

Results from calibration tests at room temperature and at 150, 250, and 350 °C are summarized in Table 5-1. As indicated in the table, room temperature tests were conducted on the bench top and in an autoclave. Results from Test 1 are shown in Figure 5-3, which are typical of the room temperature bench top data.

Table 5-1. Calibration summary.

Test	Description	Temperature (°C)	Sensitivity (mV/mm)
1	bench top	room	1672
2	bench top	room	1668
3	autoclave	room	1675
4	autoclave	150	1702
5	autoclave	250	1756
6	autoclave	350	1780

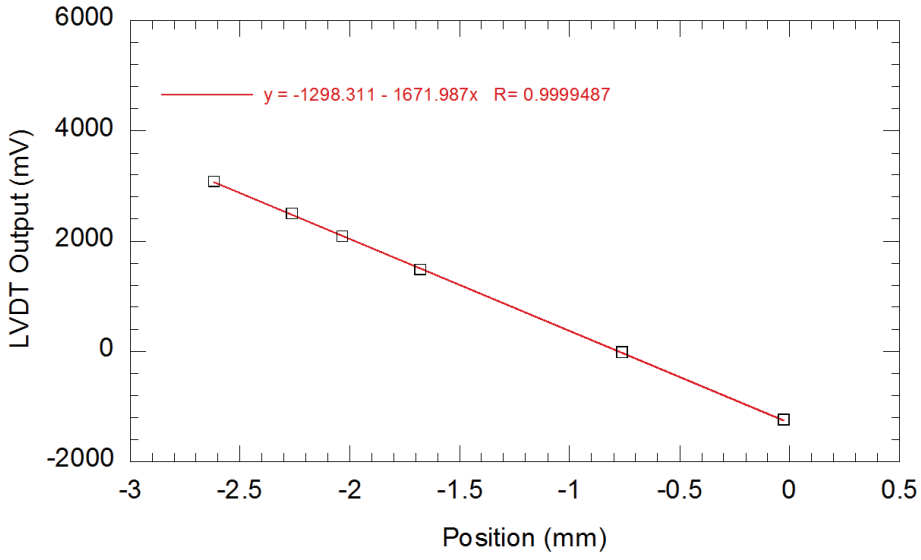

Figure 5-3. Bench top calibration results from Test 1 (at room temperature).

As indicated in Figure 5-3, the LVDT output voltage and the associated displacement were collected as the bolt was incrementally tightened (yielding a total of 6 data points in this case). A linear curve fit of the testing was performed. The slope of the line reveals the sensitivity of the LVDT. In contrast, autoclave data was limited to obtaining just two data points; one in which the travel adapter was pulled downward (with the retaining nut) to contact the top of the travel blocks and one in which bellows compression (due to autoclave pressurization) pulled the travel adapter upward to contact the bottom of the travel blocks. The resulting sensitivity was evaluated using these two data points. Regardless of these differences in the method for data collection, the room temperature results were found to be consistent. This indicates that the specialized autoclave fixture can be used to accurately collect calibration data inside the autoclave.

Averaging all room temperature calibration data yields a value of 1672 mV/mm. It is worth noting that averaging appears to be justified because differences in the measured calibration values do not translate to any appreciable discrepancy. Specifically, the maximum discrepancy for the allowable bellows travel across all room temperature data is (at most) 0.015 mm.

In addition to room temperature calibration data, measurements were also completed at 150, 250, and 350 °C as indicated in Table 5-1. Linear interpolation of this data provides a means to relate any measured LVDT output voltage to a corresponding displacement over the range of temperatures anticipated.

6. SUMMARY

Understanding the creep behavior of materials in a radiation environment is an essential aspect in evaluating safety issues associated with nuclear power plant operation, especially for nuclear power plants desiring to extend their operational lifetime. In US MTRs, this understanding has been achieved through a "cook and look" approach (where specimens are irradiated under load for some period of time and then removed from a materials test reactor for post-irradiation examination). To address the inability to obtain, real-time creep data during an irradiation, a creep test rig with an externally-pressurized bellows was developed and readied for deployment in ATR Loop 2A. As reported in this document, this original creep test rig was enhanced with the capability of internally pressurizing the bellows which enables variable strain rate testing, fatigue testing and a larger selection of test materials.

The Variable Load Creep Test Rig characterization and calibration activities have been completed to support ATR deployment. Specifically, the bellows was characterized, indicating a spring rate of 138 N/mm and an effective area of 78.3 mm. LVDT sensitivity data were obtained that span the range from cold start up conditions to those conditions typical of an operating PWR loop. Hence, the Variable Load Creep Test Rig is also ready for deployment in ATR Loop 2A.

7. REFERENCES

1. D. L. Knudson, K. L. Davis, K. G. Condie, and J. L. Rempe, "Qualification of an LVDT-Based Creep Test Rig for Use in ATR Loop 2A," INL/LTD-12-26173, Idaho National Laboratory, August 2012.

2. J. L. Rempe, D. L. Knudson, J. E. Daw, T. C. Unruh, B. M. Chase, K. L. Davis, A. J. Palmer, and R. S. Schley, "Advanced In-pile Instrumentation for Material and Test Reactors," *ANIMMA International Conference*, Marseille, France, June 2013.

3. P. Moilanen, S. Tähtinen, B.N. Singh, and P. Jacquet, "In-Situ Investigation of the Mechanical Performance and Life Time of Copper: Final report on Design, Construction, and Calibration of Test Module for In-Reactor Tensile Tests in BR2 Reactor," VTT Report BTUO 76-031127, October 27, 2004.

4. N. Singh, S. Tähtinen, P. Moilanen, P. Jacquet, and J. Dekeyser, "In-Reactor Uniaxial Tensile Testing of Pure Copper at a Constant Strain Rate at 90 °C," *Journal of Nuclear Materials*, 320, pp.299–304, 2003.

5. D. L. Knudson and J. L. Rempe, "Evaluation of LVDTs for Use in ATR Irradiation Experiments," *Sixth American Nuclear Society International Topical Meeting on Nuclear Plant Instrumentation, Control, and Human-Machine Interface Technologies,* NPIC&HMIT 2009, Knoxville, Tennessee, April 2009.

6. D. L. Knudson, J. L. Rempe, and J. E. Daw, "Evaluation of Candidate Linear Variable Displacement Transducers for High Temperature Irradiations in the Advanced Test Reactor," INL/EXT-09-16972, Idaho National Laboratory, September 2009.

7. D. L. Knudson and J. L. Rempe, "Recommendations for Use of LVDTs in ATR High Temperature Irradiation Testing," *Seventh American Nuclear Society International Topical Meeting on Nuclear Plant Instrumentation, Control and Human-Machine Interface Technologies*, NPIC&HMIT 2010, Las Vegas, Nevada, November 2010.

8. B. G. Kim, J. L. Rempe, D. L. Knudson, K. G. Condie, and B. H. Sencer, "In-Situ Creep Testing Capability Development for the Advanced Test Reactor," *Nuclear Technology*, Vol. 179, No. 3, pp.417-428, September 2012.

9. D. L. Knudson and J. L. Rempe, "Linear Variable Differential Transformer (LVDT)-Based Elongation Measurements in Advanced Test Reactor High Temperature Irradiation Testing," *Measurement Science and Technology*, Vol. 23, 025604, January 2012.

10. J. Rempe, H. MacLean, R. Schley, D. Hurley, J. Daw, S. Taylor, J. Smith, J. Svoboda, D. Kotter, D. Knudson, S.C. Wilkins, M. Guers, L. Bond, L. Ott, J. McDuffee, E. Parma, and G. Rochau, New *In-Pile Instrumentation to Support Fuel Cycle Research and Development,* FCRD-FUEL-2011-000033, (also issued as INL/EXT-10-19149), January 2011.